



Fermi National Accelerator Laboratory

FERMILAB-Conf-92/305

The DØ Muon System and Early Results on its Performance

David Hedin
for the DØ Collaboration

*Fermi National Accelerator Laboratory
P.O. Box 500, Batavia, Illinois 60510*

October 1992

Submitted to Proceedings of *XXVI International Conference on High Energy Physics*,
Dallas, Texas, August 6-12, 1992

Disclaimer

This report was prepared as an account of work sponsored by an agency of the United States Government. Neither the United States Government nor any agency thereof, nor any of their employees, makes any warranty, express or implied, or assumes any legal liability or responsibility for the accuracy, completeness, or usefulness of any information, apparatus, product, or process disclosed, or represents that its use would not infringe privately owned rights. Reference herein to any specific commercial product, process, or service by trade name, trademark, manufacturer, or otherwise, does not necessarily constitute or imply its endorsement, recommendation, or favoring by the United States Government or any agency thereof. The views and opinions of authors expressed herein do not necessarily state or reflect those of the United States Government or any agency thereof.

THE DØ MUON SYSTEM AND EARLY RESULTS ON ITS PERFORMANCE*

David Hedin for the DØ Collaboration¹

Department of Physics
Northern Illinois University
DeKalb, IL, 60115

The DØ detector is a large, general-purpose detector designed to take full advantage of the 2 TeV energy of the Fermilab collider. The design of the experiment emphasizes accurate identification, complete angular acceptance, and precise measurement of the decay products of W and Z bosons: charged leptons (both electrons and muons), quarks and gluons, which emerge as collimated jets of particles, and noninteracting particles, such as neutrinos. The primary physics goals of DØ include searching for new phenomena, such as the top quark or particles outside the standard model, and high-precision studies of the W and Z bosons. In addition, the excellent muon identification will allow the study of b -quark production and decay. This report will describe DØ's muon system, give preliminary measurements of chamber and trigger rates, and discuss muon identification.

The DØ detector is shown in Figure 1. It consists of three major hardware systems: calorimetry, muon detection, and central tracking, which together allow fairly complete characterization of most proton-antiproton collision events.² The central tracking system consists of four drift-chamber systems (vertex, central, and two end systems) and transition radiation detectors for electron identification. Surrounding the central tracking system are three uranium/liquid-argon

calorimeters. The uranium is a dense medium, allowing containment of high-energy hadron showers in a relatively short depth, as well as equal response to electrons and hadrons, while the liquid-argon ionization medium gives ease of calibration, stability, radiation hardness, and the ability to build in fine segmentation in all three coordinates. Finally, surrounding the calorimeters is the muon system,³ consisting of five iron toroids and three layers of proportional drift tube chambers.

The muon toroids are used to measure the muon momentum and absorb all remnant portions of hadron showers. The central toroid is 1.09 m thick while the ends are each 1.52 m thick. The toroids are operated with an average field of 1.9 T. The momentum resolution is dominated by multiple scattering with a typical value of 20%. The combined calorimeter plus toroid thickness varies from about 14λ in the central region to 19λ in the end regions. This thickness reduces backgrounds from hadronic punchthroughs to a negligible level,⁴ but there is still a significant singles rate in the muon chambers from hadron-induced spray.

Three layers of drift chambers, one between the calorimeter and toroid and two outside the toroid, are used to measure muon trajectories. The wide-angle muon system consists of 164 chambers, using 10 cm cells, which cover the angular region greater than about 10 degrees. These chambers combine drift time measurement with time division and vernier

*This work was supported in part by the U.S. Department of Energy and the National Science Foundation.

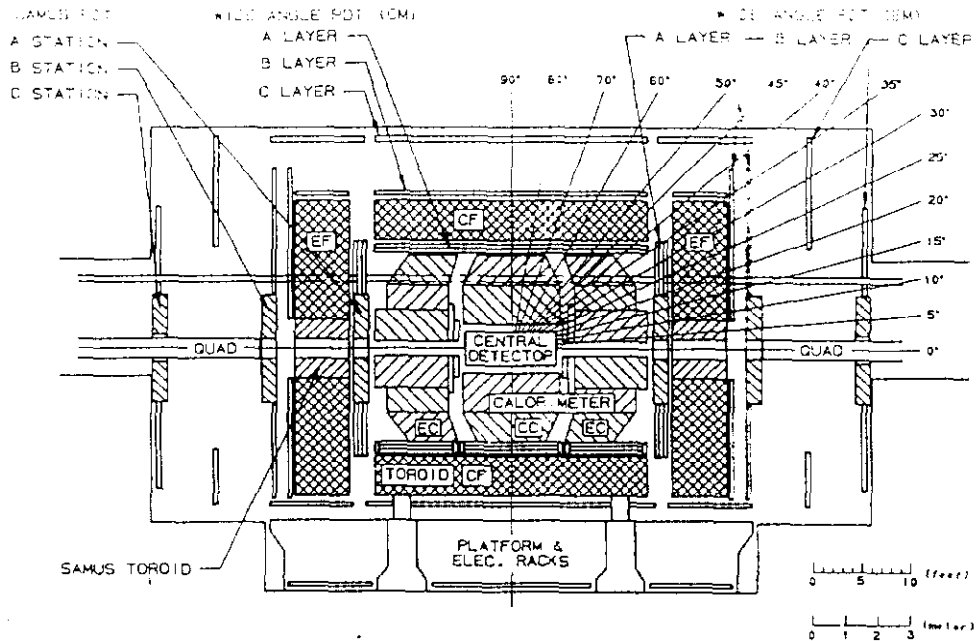


Figure 1. Elevation view of the $D\emptyset$ detector.

pads to obtain 3D points. The innermost layer has four measurement planes while the outer two have three each so that most muons are measured with ten 3D points. In the small-angle region between 5 and 20 degrees, six modules of 3.0 cm drift cells are used with each module having six planes in an XX,YY,UU configuration. The smaller cell size is needed in this region to reduce cell occupancy and to increase the p_t threshold of the trigger. Figure 2 gives the muon geometric acceptance as a function of η with the requirement that the muon goes through at least two of the three layers. The muon acceptance is greater than 70% for all $|\eta| < 3.2$. Also shown is the acceptance requiring all three layers to be hit. Gaps in the central region coverage are due to support and service structures.

There are three stages to the $D\emptyset$ muon trigger. The first two (Level 1 and 1.5) use hardware logic and fast processors to make trigger decisions in about 3.5 and 20 μsec respectively.⁵ The drift time and time division information is ignored at these stages and the hit cells are used as simple hodoscopic elements of 1.5 to 6 cell widths in Level 1 and

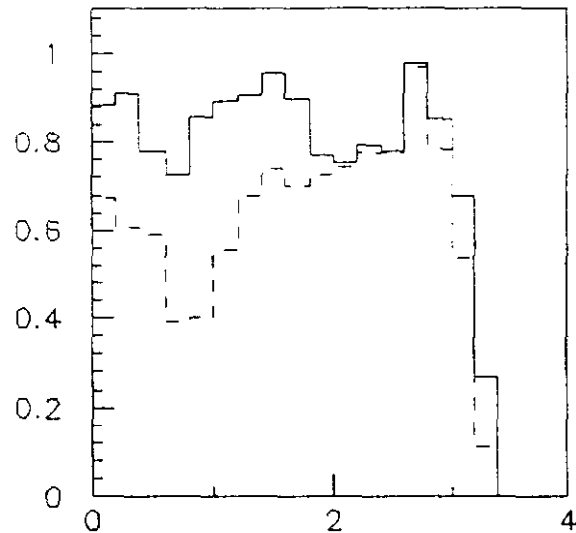


Figure 2. Muon geometric acceptance versus η for all reconstructed tracks (solid) and for 3-layer tracks (dashed).

one-half cell width in Level 1.5. The muon Level 2 trigger uses a VAX processor farm and the digitized data to reconstruct muon candidates. The Level 2 trigger is a subset of the offline reconstruction software and is designed to take about 250 ms per event. The muon-related portion of the data acquisition bandwidth will be about 400 Hz passing Level 1, 80 Hz passing Level 1.5, and 0.3 Hz passing Level 2 and then written to tape.

Level 1 triggers have two primary sources: cosmic rays in the central region and hadron-induced spray in the forward region. A set of scintillation counters covering the central ceiling is used to reduce cosmic ray triggers. Hadron-induced triggers are often due to uncorrelated hits. The average event has about 75 hits in the wide-angle chambers with most of these hits at small angles. To deal with this, smaller effective cell size is used at Level 1 at lower angles and all three layers are required to produce a valid trigger. We are currently implementing the muon trigger. As of the writing of this report we have measured a Level 1 single muon trigger rate of $10 \mu\text{b}$ and $75 \mu\text{b}$ for the regions $|\eta| < 1.0$ and $|\eta| < 1.7$ respectively. The dimuon trigger rate for $|\eta| < 1.7$ is $4 \mu\text{b}$. The Level 1.5 trigger is observed to have a further rejection factor of 2-5 and we are in the process of optimizing its use.

Muon identification utilizes information from the muon system itself, the central tracking, and the calorimeter. The primary backgrounds are from cosmic rays, which are out of time with the beam crossing and do not intercept the primary vertex, and hadron-induced spray (often uncorrelated chamber hits) which produces poorly fit tracks which also tend to miss the vertex. Good tracks in the muon chambers are defined by using appropriate track quality cuts (for example, on the χ^2 of the fit and the number of hits on the track) and that there are no muon chambers along the track without hits. The hit density is largest

at small angles and our multi-layer chamber coverage is also best in this region (with some muons hitting 24 wire chamber planes). Using only muon chamber information, we can also require that the track projects to the vertex; cuts on this can be used in the Level 2 trigger prior to analyzing the central tracking data.

The $D\bar{O}$ calorimeter is sensitive to minimum ionizing energy depositions, and the presence of such energy along the muon track helps to eliminate non-muon backgrounds. Muon chamber tracks are also matched with the central detector tracks. In addition to properly projecting to the muon chamber hits, the matched central track can be required to have a good fit and small impact parameter. This aids in eliminating non-muon and cosmic backgrounds, and can also tag π/K decays. Finally, timing information in the central tracking, the muon chambers, and the scintillation counters on the central top can be used to remove any remaining cosmic ray muons.

Figure 3 shows an event display of a dimuon event a jet near each muon. The tracks reconstructed in the muon chambers project to the vertex, to minimum ionizing energy in the calorimeter, and to tracks in the central tracking system. The muon system is relatively clean both near the jets and in the angular regions closer to the beam.

After the initial three months of data collection at the Fermilab $p\bar{p}$ collider, we have found that the muon system has performed to its design expectations. The chambers are able to operate in the collision hall without any abnormal failures. The chamber rates are reasonable, agreeing within a factor of ± 2 with Monte Carlo predictions, as are the trigger rates. Triggering on muons at low angles and low p_t is still a difficult problem, and we are in the process of optimizing the trigger settings. We are also still working on our initial calibration of electronic channels and alignment from survey values so that physics processes

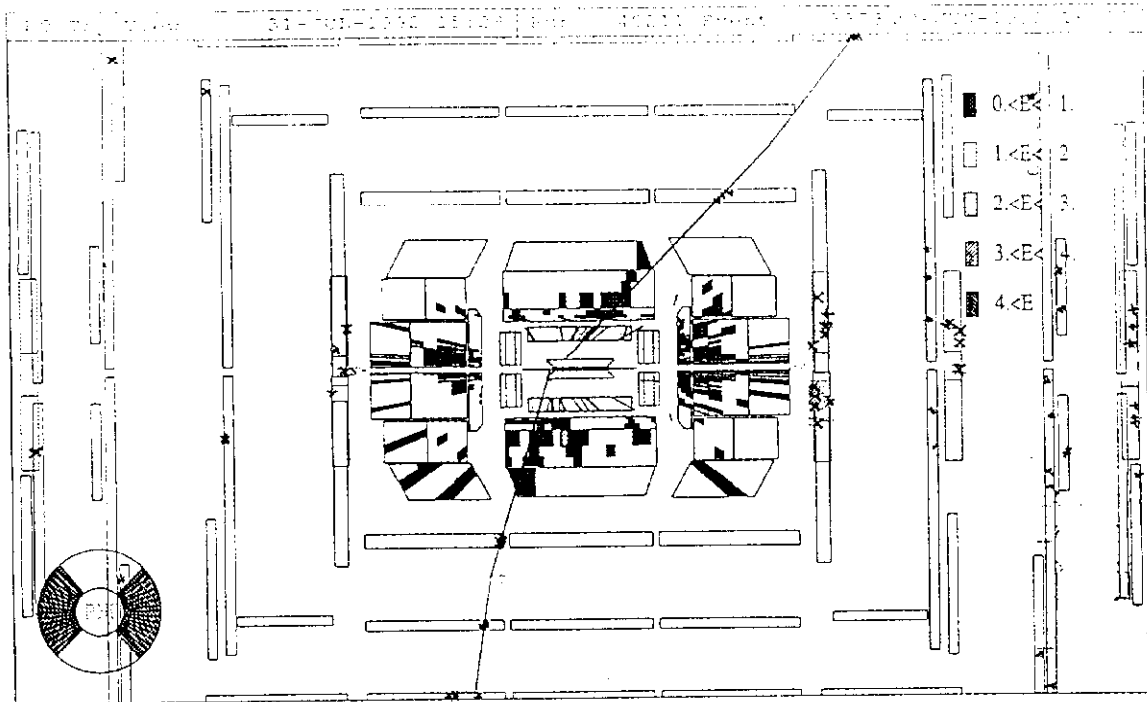


Figure 3a. Top view of a dimuon candidate event

can be searched for and studied at the earliest possible date.

REFERENCES

1. Uniandes, Arizona, Brookhaven, Brown, California-Riverside, CBPF, CINVESTAV, Columbia, Delhi, Fermilab, Florida State, Hawaii, Illinois-Chicago, Indiana, Iowa State, LBL, Maryland, Michigan, Michigan State, Moscow State, NYU, Northeastern, Northern Illinois, Northwestern, Notre Dame, Panjab, IHEP-Protvino, Purdue, Rice, Rochester, CEN-Saclay, Stony Brook, SSCL, Tata Institute, Texas-Arlington, Texas A & M.
2. *DØ Design Report*, Fermilab (1984).
3. C. Brown, et al., *NIM*, A279, 331 (1989); J.M. Butler, et al., *NIM*, A290, 122 (1990).
4. D. Green, et al., *NIM*, A244, 356 (1985).
5. M. Fortner, et al., *IEEE Transactions on Nuclear Science*, 38, 480 (1991).

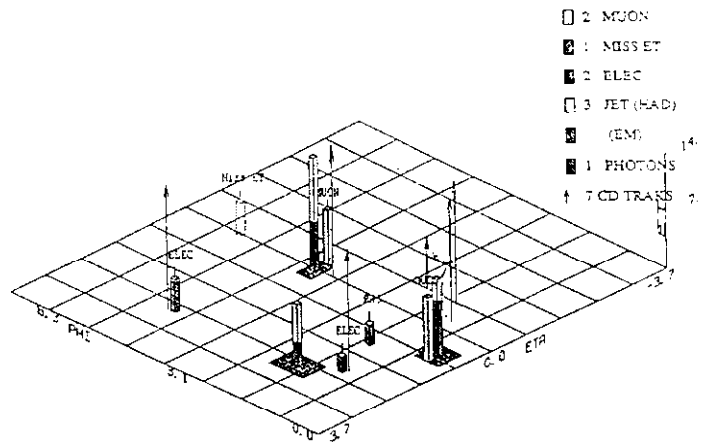


Figure 3b. Lego plot (in η and ϕ) of a dimuon candidate event.